JOURNAL OF MATERIALS SCIENCE 2 (1967) 332–338

Three-Stage Hardening in Tantalum Deformed in Compression

B. L. MORDIKE, G. RUDOLPH*
Department of Metallurgy, The University, Liverpool, UK

Received 13 January 1967

High-purity tantalum single crystals were deformed in compression at various temperatures and strain rates. The shape of the stress/strain curve is strongly dependent on orientation, but, for certain orientations, the stress/strain curve could be divided into three stages for tests conducted over a narrow range of temperatures and strain rates. The work-hardening rates for the various stages were determined and compared with those obtained by other workers. Strain-rate-change and temperature-change experiments were evaluated to yield values of activation energy and activation volume. The values obtained were comparable with those obtained in other investigations on polycrystalline tantalum or on single crystals where three-stage hardening was not observed.

1. Introduction

The fundamental study of the mechanical properties of bcc metals has been made difficult by the extreme sensitivity of these metals to impurities. It has not yet been established whether impurities cause the sharp increase in yield stress with decreasing temperature [4], or whether this is an intrinsic property of the bcc lattice [9, 10]. The stress/strain curve shape cannot be predicted as it can for fcc metals. Until quite recently, it was accepted that bcc metals exhibit a parabolic stress/strain curve. However, within certain limits of purity, orientation, temperature, and strain rate, it has been established that the stress/strain curve can be subdivided into stages, and an attempt has been made to correlate these with three-stage hardening in fcc metals [11].

The effect has hitherto been studied in tension, and thus the full extent of the stages of hardening are not appreciated, particularly at low temperatures. The reason for this is that, in tension, plastic instability on yielding and consequent premature necking occur. This behaviour is a result of the high yield stress and low work-hardening rate. Since the yield stress rises sharply with decreasing temperature, and the work-hardening rate remains unchanged or even decreases, the effect becomes more marked at low temperatures. Only by conducting compression tests is it possible to obviate this phenomenon.

The present work describes compression tests carried out on tantalum single crystals over the temperature range 77 to 573° K. The object was to establish the deformation parameters in compression for an orientation exhibiting various hardening stages; so that in a later investigation the effect of alloying could be established. Of particular interest were the critical resolved shear stress, the length of the various stages, and their rates of work-hardening.

2. Experimental Details

The tantalum used in this investigation was provided, in the form of sintered rods, by CIBA Ltd, Basle. First the rods were given an outgassing anneal in vacuum; following which, single crystals were produced by electron-beam zone melting. Two orientations, produced by seeding, are referred to as orientations a and b. Crystals with orientation a (see fig. 1) were used throughout this work, except where otherwise stated. Orientation b is shown in fig. 2. Each crystal was zoned six times at a speed of 0.5 cm/min. The pressure for the final pass was better than 1×10^{-5} torr. The analysis of the tantalum before and after electron-beam melting is given

*Now at Metallgesellschaft, Frankfurt, West Germany.

in table I. The analysis was performed by CIBA Ltd. Other impurities were present only as traces; with the exception of niobium, of which there was 400 ppm.

TABLE I Analysis of interstitial elements in tantalum.

	ppm by weight			
	H	O	N	C
Starting material	5	72	28	3.5
Zone-refined crystals	2	9	< 1	5

The crystals were cut directly from the zoned rods. Sensitive control of the zoning conditions ensured that the variation in diameter along the length of a specimen was less than 0.05 mm and that the ellipticity was less than 0.1 mm. The final specimen size was 12 mm long and 4 mm diameter – a ratio of length to diameter of 3:1. The end surfaces of the compression specimens were polished with fine emery paper. A polishing jig ensured perfectly parallel ends.

Deformation took place in an Instron Universal testing machine. The temperatures were obtained using the baths given in table II.

TABLE II Temperature baths used for temperatures between +300 and −196° C.

Temperature (°C)	Bath
100 to 300	Oil
0 to 100	Water
0 to −72	Alcohol and carbon dioxide
−72 to −131.5	Isopentane, cooled by liquid nitrogen
−196	Liquid nitrogen

3. Evaluation of Results

The results were evaluated for slip on the $(\bar{2}11)$ $<111>$ and $(\bar{1}01)$ $<111>$ systems for orientations a and b respectively [1]. There is still no overall agreement as to the operative slip systems for bcc metals, but it is considered that the majority of the evidence supports (211) as well as (110) slip. The stress/strain curves were evaluated by computer, using the following formulae for converting load and extension to stress (τ) and shear glide (a) [2].

$$\tau = \left(\frac{L}{A_0}\right)\left(\frac{l}{l_0}\right)^2 \left\{\cos\lambda_0 \left[1-\left(\frac{l}{l_0}\right)^2 \sin^2 x_0\right]^{\frac{1}{2}}\right\}$$

$$a = \{[(l/l_0)^2 - \sin^2 x_0]^{\frac{1}{2}} - \cos x_0\}/\cos\lambda_0$$

where: L is the load; A_0, the initial cross-sectional area; l_0, the initial length of the specimen; l, $l = l_0 - \Delta l$, Δl being the reduction in length; x_0, the angle between the glide-plane normal and the specimen axis; λ_0, the angle between the slip direction and the specimen axis. These equations are valid for the case of single glide.

4. Experimental Results

4.1. Continuous Deformation

The stress/strain curves for single crystals deformed in compression are given in figs. 1 to 3. Fig. 1 shows stress/strain curves obtained over the temperature range 77 to 373° K. This orientation, a, is particularly suitable for the observation of three-stage hardening. The

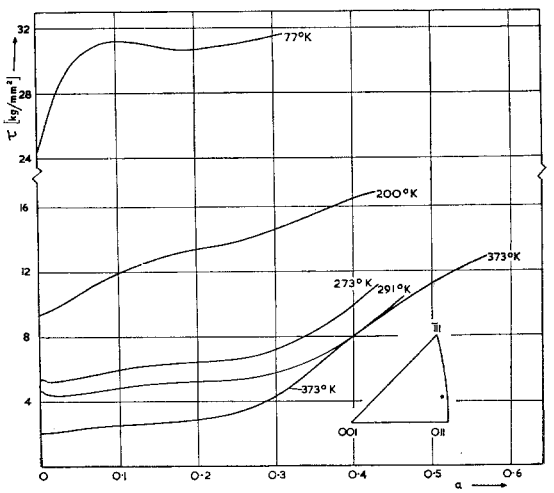

Figure 1 Typical stress/strain curves for tantalum single crystals deformed at different temperatures.

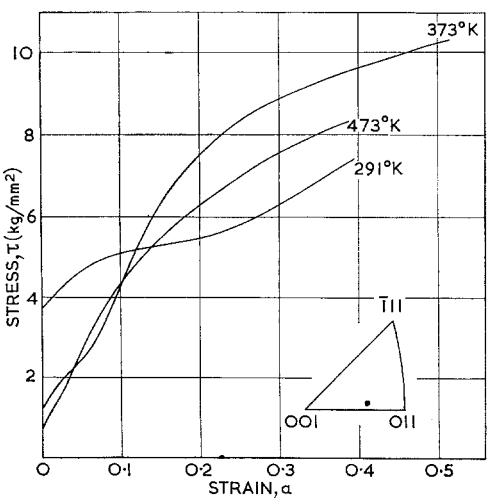

Figure 2 Stress/strain curves for a second orientation.

strong effect of orientation on the yield stress and on the shape of stress/strain curve is illustrated in fig. 2, by presenting stress/strain curves for a second orientation, b. Although this orientation is not far removed from the a orientation, the shape of the curves has changed markedly becoming pronouncedly parabolic. When the shape of the stress/strain curve varies with orientation of the crystals and strain rate and temperature, it is difficult to decide on what value of stress to take for the yield stress. This decision is complicated further by yield points and work-softening effects. In those cases where a yield point occurs, the lower yield point, and not the upper yield stress or the extrapolation of the stress/strain curve onto the elastic portion, was defined as the flow stress; otherwise, the extrapolated value was taken. The tendency to form three stages increases with decreasing temperature, although the length of stage I would appear to decrease with decreasing temperature. Fig. 3 shows the effect of strain rate on the stress/strain curve and in particular on the critical resolved shear stress and length of stage I. Contrary to expectation, the length of stage I was found to increase with decreasing strain rate, thus being the opposite to fcc metals. Since the length of the various stages can be dependent on the specimen size and mode of deformation, an absolute comparison with other workers is difficult.

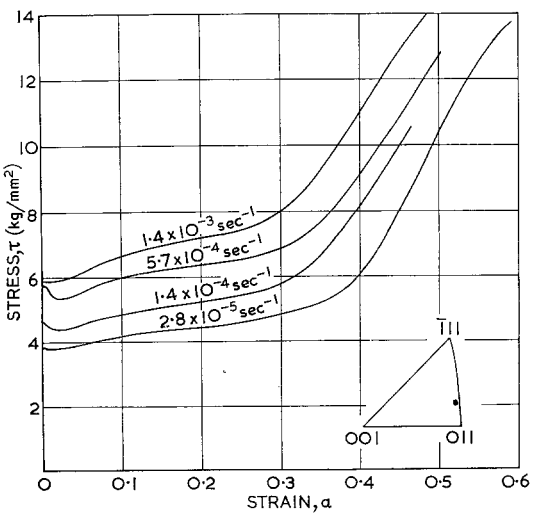

Figure 3 Effect of strain rate on stress/strain curves.

The temperature and strain-rate sensitivity of the work-hardening rates θ_I and θ_{II} are given in figs. 4 and 5 respectively. θ_{II} passes through a maximum at about 350° K. θ_I, however, decreases slightly with increasing temperature. θ_{II} decreases with increasing strain rate; θ_I increases very slightly.

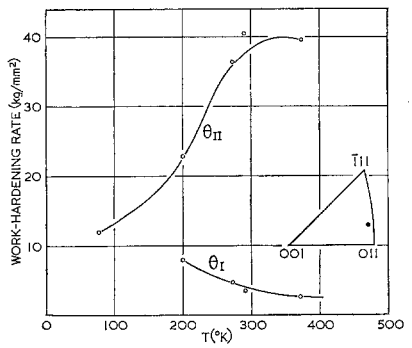

Figure 4 Work-hardening rates θ_I and θ_{II} for a range of temperatures.

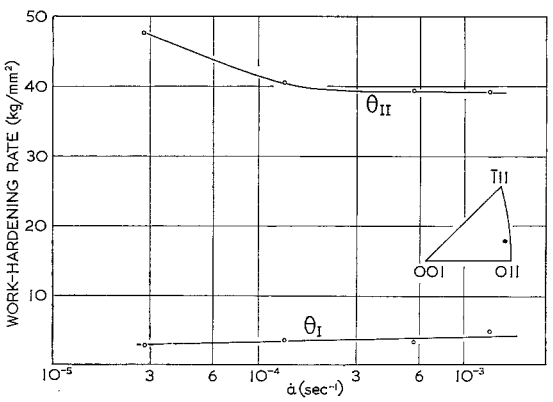

Figure 5 Dependence of work-hardening rate on strain rate.

4.2. Temperature and Strain Rate Change Experiments

Temperature and strain rate change experiments [7, 3, 8], particularly in stage I, enabled the temperature and strain-rate sensitivity of the flow stress to be investigated with relatively few crystals. The critical resolved shear stress is generally divided into two contributions, τ_G and τ^*,

$$\tau_0 = \tau_G + \tau^* \qquad (1)$$

τ_G is the minimum stress which must be applied to cause plastic deformation. It is a friction stress and is defined as the limiting value of the critical resolved shear stress for infinitely small shear strain rates $\dot{\alpha}$.

$$\tau_G \to \tau_0 \text{ as } \dot{a} \to 0 \qquad (2)$$

τ^* is the additional shear stress for $\dot{a} > 0$. In part, it can be provided by thermal fluctuations.

The relationship of τ^* with T and $\dot{a}$ is usually described by an "Arrhenius" equation:

$$\dot{a} = \dot{a}_0 \exp\left(-U(\tau^*)/kT\right) \dagger \qquad (3)$$

$\dot{a}_0$ is a frequency factor which is determined by the dislocation density and obstacle density.

The customary description of the stress dependence of the activation energy U is

$$U(\tau^*) = U_0 - v(\tau^*) \qquad (4)$$

If (3) is treated in the same manner as a thermodynamic equation of state, one can, by choosing, for example, τ^* and T as independent thermodynamic quantities, develop a thermodynamics of deformation. If one assumes that the temperature dependence of τ_0 is contained solely in τ^*, and that U_0 and $\ddot{a}_0$ are constants, then, by partial differentiation of τ^* with respect to T and $\dot{a}$, one obtains

$$U(\tau^*) = -kT^2 \left(\frac{\partial \tau^*}{\partial T}\right)_{\dot{a}} \left(\frac{\partial \ln \dot{a}}{\partial \tau^*}\right)_T \qquad (5)$$

$$v^* = v + \tau^* \frac{\partial v}{\partial \tau^*} = \left(\frac{\partial \ln \dot{a}}{\partial \tau^*}\right)_T \qquad (6)$$

v^* is termed the effective activation volume. By conducting strain-rate-change or temperature-change experiments, it is possible to separate the τ^* and τ_G contributions to the flow stress. In such an experiment, the specimen is deformed up to a certain point, and then the strain rate or temperature is changed. A different stress is required to continue deformation, and the difference $\Delta\tau$ is determined. The flow stress is thus measured at two temperatures or two strain rates for the same dislocation configuration. $\Delta\tau$ is thus equal to $\Delta\tau^*$.

Fig. 6 shows the change in flow stress for a change in temperature. The curve is, in effect, the temperature dependence of the yield stress in differentiated form. Graphical integration based on the room-temperature value of τ_0, which was the mean of seven direct readings, gives the curve shown in fig. 7. The τ_0 points lying on the curve were measured directly, the mean of two or three readings being taken. Thus good agreement was achieved between the temperature dependence of τ_0 obtained from temperature-change experiments and that measured directly using several crystals.

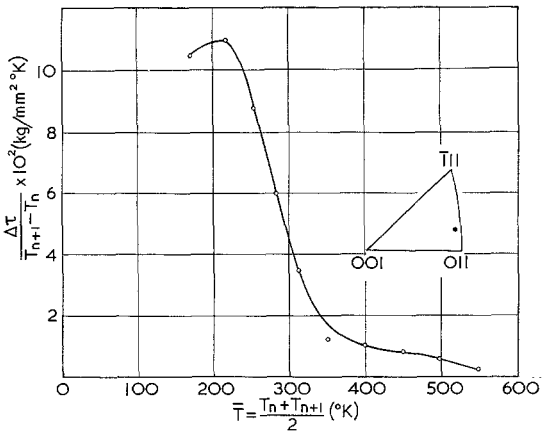

Figure 6 Change in flow stress for a change in temperature.

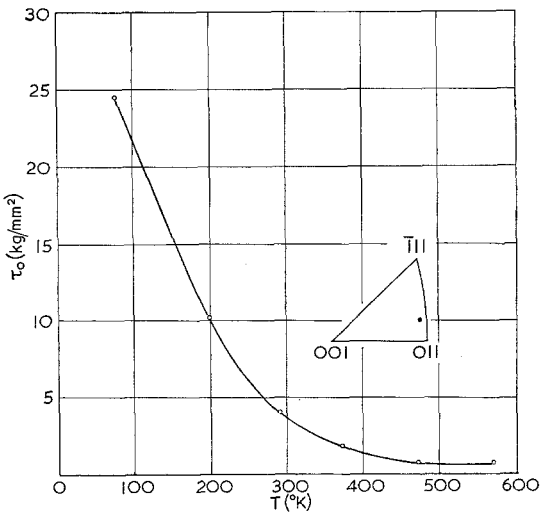

Figure 7 Temperature dependence of the initial flow stress.

The results of the strain-rate-change experiments are presented in fig. 8. The change in flow stress depended on the magnitude of the strain-rate change and also on the basic strain-rate value $\dot{a}_G$. $\Delta\tau$ was independent or only slightly dependent on strain in stage I, where all the strain-rate changes were performed.

5. Discussion

The present experiments were not undertaken to study specifically the temperature dependence of the flow stress. For this, additional experi-

†Strictly speaking one should use the free energy of activation ΔG instead of the activation energy U.

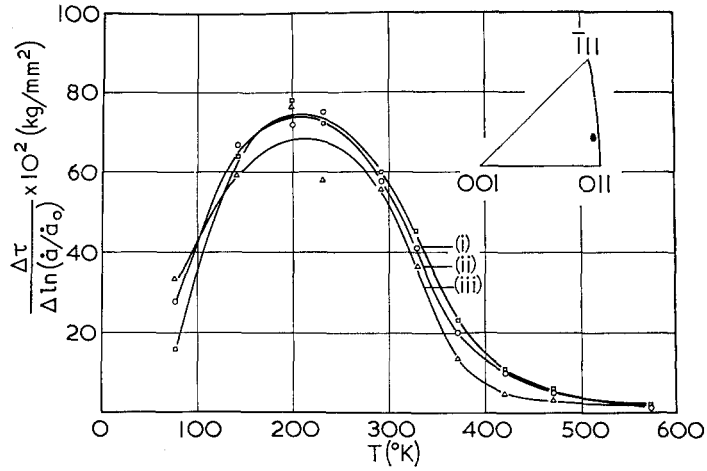

Figure 8 Strain-rate sensitivity of tantalum as a function of temperature. Curve (i) factor 10, $\dot{a}_G = 1.4 \times 10^{-4}$ sec^{-1}. Curve (ii) factor 4, $\dot{a}_G = 1.4 \times 10^{-4}$ sec^{-1}. Curve (iii) factor 5, $a_G = 2.8 \times 10^{-5}$ sec^{-1}.

ments at lower temperatures are required. The emphasis was placed on establishing the extent of three-stage hardening in compression. The number of specimens required for the investigation was considerably reduced by conducting strain-rate-change and temperature-change experiments. In addition to giving the required information, the change experiments can be evaluated to determine the activation energy and activation volume [7]. Figs. 9 and 10 illustrate the evaluation of the activation energy

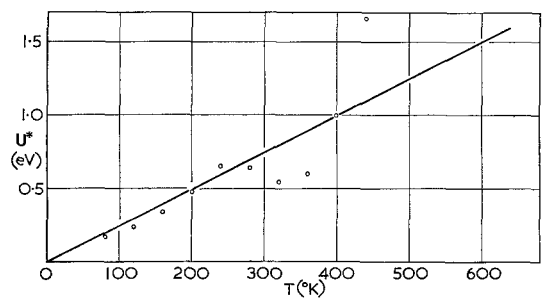

Figure 9 Activation energy U^* for deformation plotted against temperature.

U_0 and the stress dependence of the activation volume. The activation energy U_0 was calculated from the basic equation

$$U_0 = kT_0 \ln (\dot{a}_0/\dot{a})$$

as 1.4 eV, taking $T_0 = 600°$ K from fig. 9, and $\dot{a}_0 = 3.6 \times 10^7$ as evaluated from the slope of U^* versus T. The activation volume decreases rapidly with stress from 25×10^{-21}cm^3 ($1050b^3$) at $\tau = 0.7$ kg/mm^2 to 0.3×10^{-21} cm^3 ($13b^3$) at $\tau = 25$ kg/mm^2 (where b is the Burgers vector).

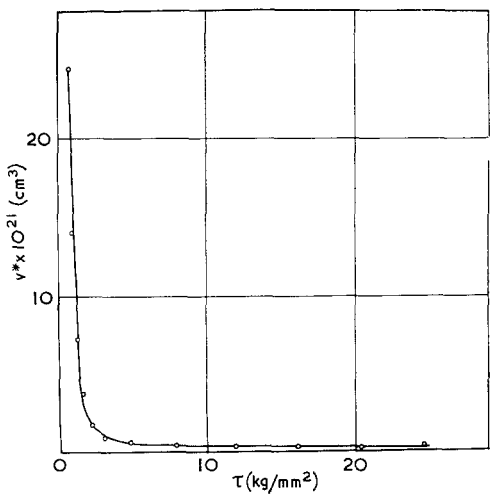

Figure 10 Activation volume as a function of applied stress.

The evaluation was based upon the Arrhenius rate equation and was carried out in the conventional manner. Certain criticisms can be levelled against the thermal activation analysis, and it is considered best to restrict the discussion to the comparison of these results with those evaluated in a like manner, and not to base discussion of deformation mechanisms on the rate-change experiments alone.

Three-stage hardening was observed in tantalum in compression for orientation a, similar to that obtained in tantalum [5] and niobium [11] in tension and niobium in compression [12]. Three-stage hardening was observed down to the lowest temperatures investigated. Stage I was generally linear, although, at temperatures

below 200° K, it was preceded by a long parabolic stage. In the case of fcc metals, the lengths of stages I and II, a_{II} and a_{III} respectively, increase with decreasing temperature or increasing strain rate; this behaviour has also been reported for bcc metals [5]. This has been explained in terms of stage I being limited by the interaction of primary dislocations with those on other planes forming sessile dislocations. This process may be assisted by temperature: hence increasing the temperature would cause a decrease in the length of stage I. In the present investigation, the length of stage I decreased with decreasing temperature or increasing strain rate over the whole temperature and strain-rate range. Similar behaviour was observed for tantalum in tension at temperatures below 273° K. No three-stage hardening was observed for orientation b, although, at 291° K, the parabolic curve typical of this orientation began to break up. The present investigation not only shows that the dependence of a_{II} on temperature and strain rate is different from that for fcc metals, but also shows that θ_I, the work-hardening rate, behaves differently (i.e. increases with decreasing temperature or increasing strain rate). This behaviour is perfectly consistent in itself, but makes the explanation in terms of the formation of sessile dislocations difficult. The value of θ_I is higher than the values published by Mitchell and Spitzig [5] for tantalum crystals oriented near the centre of the standard triangle. It is in reasonable agreement, however, with the values obtained for niobium deformed in compression [12], which are themselves also higher than the corresponding ones measured in tension [1]. The effect of the type of deformation, compression or tension, is not completely known for bcc metals, but, for fcc metals, Haasen *et al* found that the stress/strain curves for iridium deformed in tension and compression were identical up to 15% shear strain [6]. It would have been reasonable to expect this to be the case for bcc metals, so long as the same slip system is operative in both types of deformation. The low work-hardening rate in stage I may be associated with the predominantly single slip. Some secondary slip was observed initially in stage I, but this soon gave way to single slip. The length of stage I is influenced very much by the length of the specimen; the friction at the plattens also has an effect. Consequently, no comparison of the actual length of stage was made with results from other sources. The somewhat higher values of θ_I, obtained by Taylor and ourselves for specimens deformed in compression, may well be due to the relatively short specimen and the effect of the plattens on the operation of some other slip systems.

In some cases, a rounded yield point or period of softening was observed in stage I. This could be due to the limited amount of non-primary slip decreasing or annihilation of jogs.

In stage II, $\theta_{II}/G \approx 1/200$, where G is the shear modulus. This is somewhat higher than previously found for tantalum, but it lies within the range found for fcc metals. Various work-hardening mechanisms have been discussed for bcc metals [11] and it is not proposed to elaborate on them here, since no conclusions can be made.

Stage III was observed, but in most cases the tests were discontinued in stage II, as deformation at high strains in compression is not easy. Since many slip lines are observed throughout the deformation, stage III cannot be associated with the onset of cross-slip as in fcc metals. Some other mechanism of work-softening must operate.

6. Conclusions

Three-stage hardening has been observed in tantalum deformed in compression over a wide range of temperatures and strain rates. The temperature dependence of the flow stress and the activation parameters agree with those found by other workers. However, some differences in the behaviour in stage I were observed: the length decreased with decreasing temperature or increasing strain rate, whereas the work-hardening rate increased slightly with decreasing temperature.

Acknowledgements

This work was sponsored by the Ministry of Aviation and their support is gratefully acknowledged. It was carried out in the Department of Materials Science, University College of North Wales, Bangor.

References

1. B. L. MORDIKE, *Z. Metalk.* **52** (1961) 587.
2. E. SCHMID and W. BOAS, "Kristallplastität" (Springer, Berlin, 1936).
3. B. L. MORDIKE and P. HAASEN, *Phil. Mag.* **7** (1961) 459.
4. R. BURBACH, B. L. MORDIKE, and P. HAASEN, *J. Iron Steel Inst.* **204** (1966) 390.

5. T. E. MITCHELL and W. SPITZIG, *Acta Met.* **13** (1965) 1169.
6. P. HAASEN, H. HIEBER, and B. L. MORDIKE, *Z. Metalk.* **56** (1965) 833.
7. H. CONRAD and H. WIEDERSICH, *Acta Met.* **8** (1966) 128.
8. B. L. MORDIKE, *Z. Metalk.* **9** (1962) 587.
9. B. C. MASTERS and J. W. CHRISTIAN, *Proc. Roy. Soc. A* **281** (1964) 223.
10. H. CONRAD, *J. Iron Steel Inst.* **198** (1961) 365.
11. T. E. MITCHELL, R. FOXALL, and P. B. HIRSCH, *Phil. Mag.* **8** (1963) 95 and 1865.
12. G. TAYLOR and J. W. CHRISTIAN, *Acta Met.* **13** (1965) 1216.